

Distributed MEMS Transmission Lines for Tunable Filter Applications

Yu Liu, Andrea Borgioli, Amit S. Nagra, Robert A. York

Electrical and Computer Engineering Department, University of California at Santa Barbara, Santa Barbara, California 93106

Received 23 October 2000; accepted 28 March 2001

ABSTRACT: This paper describes the design and fabrication of a distributed MEMS transmission line (DMTL), used to realize a transmission-line with a voltage-variable electrical length for microwave circuits. The DMTL is a coplanar waveguide periodically loaded with continuously-variable MEMS capacitors. A tunable bandpass filter was designed and fabricated on 700 μm thick glass substrates using three capacitively coupled DMTL sections as variable shunt resonators. The measured results demonstrate a 3.8% tuning range at 20 GHz with 3.6 dB minimum insertion loss. Issues for future improvement are discussed. © 2001 John Wiley & Sons, Inc. *Int J RF and Microwave CAE* 11: 254–260, 2001.

Keywords: distributed circuit; MEMS; tunable filter

I. INTRODUCTION

Radio frequency microelectromechanical systems (RF MEMS) concepts have been successfully applied in the past few years to the development of low-loss RF switching devices [1–4]. The basic principle of operation is to actuate the movement of a thin metal membrane by electrostatic force when DC bias is applied between the membrane and a bottom electrode. While initially designed for RF switching operations, these devices can also act as variable capacitors when bias voltages less than pull down voltage are applied. RF MEMS capacitive devices have demonstrated some advantages in comparison to other switching and varactor devices such as lower loss, lower parasitics, and higher linearity. These advantages may offset the slow switching speed, high control

voltages, and packaging costs associated with these devices in some applications.

MEMS capacitive devices have recently been investigated for low-loss and high-performance microwave control circuit applications. In this work, we consider a possible implementation of a tunable filter structure using variable MEMS capacitors. Tunable bandpass filters are a crucial component in a variety of radar and communication systems. While existing tunable filters are fabricated using YIG resonators, active inductors, and semiconductor varactor diodes [5], improvements in MEMS technology have made it possible to use MEMS variable capacitors instead [6]. Recently, the distributed MEMS transmission line (DMTL) technique has been used to implement very low-loss millimeter-wave true-time delay phase shifters [7]. These structures provide electronically-variable phase and group velocity (and hence phase or time delay) through voltage-control of the MEMS loading capacitance. This technique can also be used to design tunable resonators, using a capacitively-coupled DMTL. The center frequency of this resonator is determined

Correspondence to: Y. Liu; e-mail: yuliu@scully.ece.ucsb.edu.

Contract grant sponsor: Air Force Research Laboratory.

Contract grant number: F19628-99-C-0017.

Contract grant sponsor: DARPA.

Contract grant number: DABT63-98-1-0006.

approximately by the frequency at which the resonators become a half wavelength long, and can be tuned by electronically varying the loading capacitance of MEMS devices.

The layout of this paper is as follows. First, the basic principle of operation of DMTL and DMTL-based resonators is described. DMTL-based tunable resonators show a wide tuning range of resonant frequency with respect to the variation of loading MEMS capacitance. A design method and relevant equations of mm-wave tunable bandpass filter based on DMTL resonators are presented. The detailed fabrication process is then discussed and followed by RF measurements.

II. PRINCIPLE OF DMTL RESONATORS

The DMTL is comprised of a high-impedance transmission line ($> 50 \Omega$) periodically loaded with MEMS variable capacitors as shown in Figure 1. The Bragg frequency (f_{Bragg}) for this periodic structure is given by:

$$f_{\text{Bragg}} = \frac{1}{\pi \sqrt{L_T (C_T + C_{\text{MEMS}})}} \quad (1)$$

where L_T and C_T are the inductance and capacitance per unit length of the unloaded line. For frequencies well below the Bragg frequency, the DMTL can be treated as a synthetic transmission line whose capacitance per unit length has been increased due to the periodic loading of MEMS capacitors [8]. The characteristic impedance (Z_L) and phase velocity (v_{phase}) of the synthetic trans-

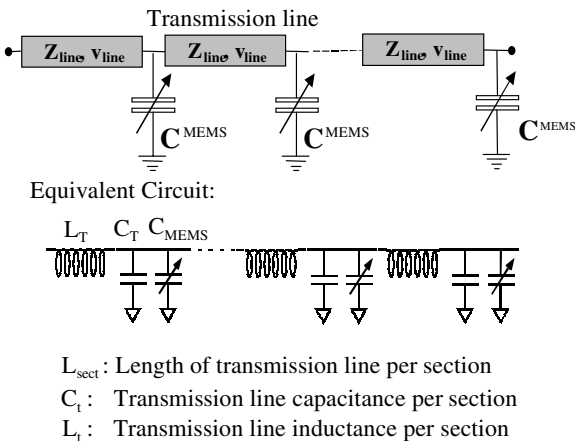


Figure 1. Schematic and equivalent circuit of a DMTL.

mission line are given by

$$Z_L = \sqrt{\frac{L_T}{(C_T + C_{\text{MEMS}})}} \quad (2)$$

$$v_{\text{phase}} = \frac{L_{\text{sect}}}{\sqrt{L_T (C_T + C_{\text{MEMS}})}} \quad (3)$$

At any given frequency, the phase shift of a DMTL with n sections is given by

$$\phi = 2\pi f n \frac{L_{\text{sect}}}{v_{\text{phase}}} \quad (4)$$

Equations (3) and (4) indicate that the variation of loading MEMS capacitance will change the phase shift and thus the electrical length of the DMTL. A DMTL-based tunable resonator is proposed as shown in Figure 2, where a DMTL section is connected to input and output ports with two coupling capacitors. To a first order approximation (neglecting loading effects) the center frequency is determined by the frequency at which the resonators become half wavelength long. From Eq. (4), the resonant center frequency of a DMTL resonator is

$$\omega_r = \frac{\pi v_{\text{phase}}}{n L_{\text{sect}}} \quad (5)$$

From the above equation, the tuning range of a MEMS tunable resonator can be deduced as follows:

$$\frac{\Delta \omega_r}{\omega_r} = 1 - \sqrt{\frac{1 + \frac{C_{\text{MEMS},0}}{C_T}}{1 + y \frac{C_{\text{MEMS},0}}{C_T}}} \quad (6)$$

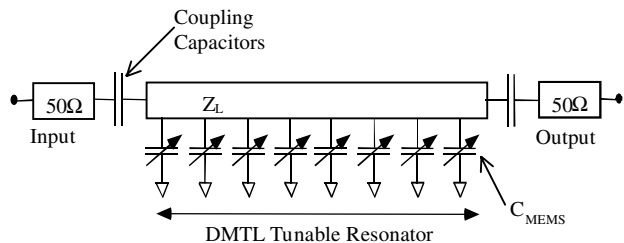


Figure 2. Topology of a DMTL-based tunable resonator.

where $C_{\text{MEMS},0}$ is the zero-bias MEMS capacitance and y is the tuning factor of the MEMS variable capacitor, defined as the ratio of the maximum-to-minimum capacitance. Fundamental electrostatic considerations limit y to a maximum of 1.5 for a simple capacitive membrane.

The DMTL tunable resonator in coplanar waveguide (CPW) form was simulated with the Agilent advance design system (ADS) software for a glass substrate ($\epsilon_r = 5.7$). L_{sect} and n are chosen to be $260 \mu\text{m}$ and 12, respectively. The coupling capacitance is 15 fF. The simulated S_{21} of DMTL tunable resonators is plotted in Figure 3 for a variety of capacitance values. The resonant frequency can be tuned effectively from 24 to 18.9 GHz with loading MEMS capacitances C_{MEMS} vary from 0 fF to 18 fF. The quality factor (Q) of the resonator is determined mostly by the CPW line since MEMS devices show very low loss. Substrate leakage needs to be avoided in high- Q DMTL tunable resonator applications.

III. MEMS TUNABLE FILTERS DESIGN

The tunable filter topology is shown in Figure 4(a) and is a modification of the capacitive gap-coupled transmission line filters. Filters of this type are commonly used as narrow bandpass filters. Each section of line is approximately one-half wavelength long at the passband center frequency and the coupling capacitors are chosen to give the correct bandwidth.

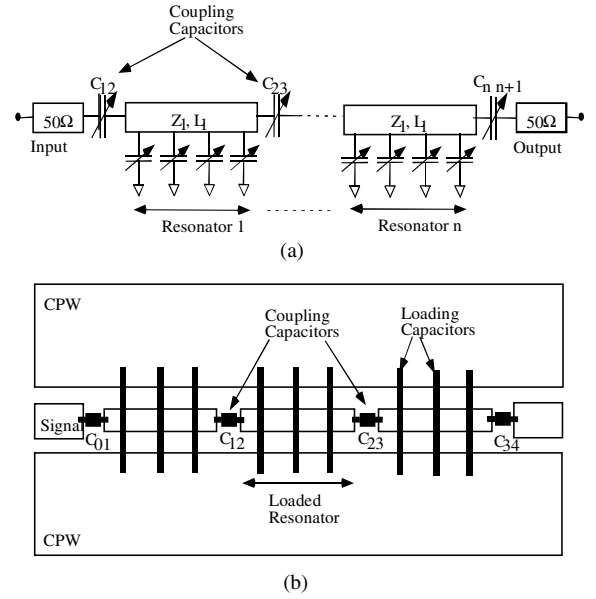


Figure 4. (a) Topology of capacitively coupled tunable filter based on DMTL resonators. (b) Layout of three-section tunable filter in coplanar-waveguide form.

The bandpass tunable filter shown in Figure 4 (b) is based on a generalized design method for capacitively coupled resonators [9]. A three-pole resonator topology is chosen for good passband to out-of-band rejection ratio. The center frequency is designed to be 20 GHz. Following a standard procedure, the coupling capacitances ($C_{i-1,i}$) and electrical length (l_{elec}) of each resonator are given in Table I.

Each resonator is a DMTL section with a Bragg frequency much higher than the designed working frequency range. Thus the synthetic transmission line approach can be used in this design [8]. The loading factor (x), defined in eq. (7), is the ratio of maximum varactor capacitance to the transmission line capacitance (C_T) per unit length.

$$x = \frac{C_{\text{var}}^{\text{max}} / L_{\text{sect}}}{C_T} \quad (7)$$

TABLE I. Summary of $C_{i-1,i}$ and l_{elec}

i	$C_{i-1,i}$ (fF)	$l_{\text{elec},i}$
1	43.04	162.03°
2	10.56	172.44°
3	10.56	162.03°
4	43.04	

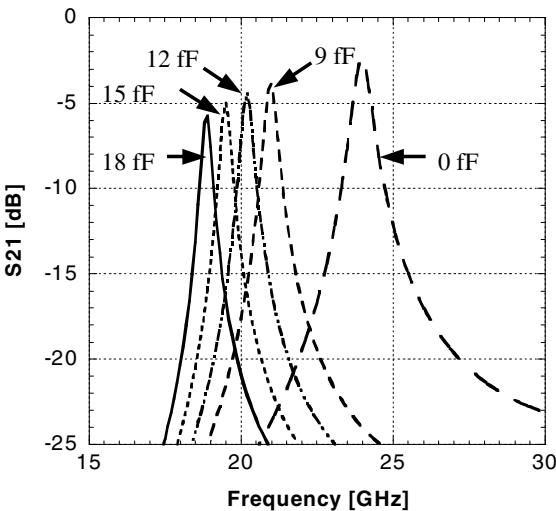


Figure 3. Simulated S_{21} of DMTL tunable resonators with loading MEMS capacitances C_{MEMS} vary from 0 fF to 18 fF.

where L_{sect} is the spacing between two adjacent periodically loaded MEMS capacitors.

While the loading factor x is selected to be larger when a wider tuning range is desired, it should also be noted that x needs to be within a certain range for input match considerations. This is because the impedance of the loaded lines used to implement the tunable resonators is also a function of the loading capacitance as shown in eq. (2). If a large change in the center frequency is attempted by using bigger variable capacitors in the resonator or by changing the variable capacitors by larger amounts, then the return loss performance will suffer due to change in filter impedance. In this design, loading factors of all resonators are chosen to be 0.5. When the characteristic impedance of a synthetic transmission line is set to 50Ω , the characteristic impedance (Z_i) of the unloaded line is

$$Z_i = 50\sqrt{1+x}. \quad (8)$$

Thus, the loading capacitance (C_{var}) and number of sections (n) in each resonator are given by

$$C_{\text{var}} = \frac{x}{50\pi f_{\text{Bragg}}(1+x)} \quad (9)$$

$$n = \frac{f_{\text{Bragg}}}{f_0} \frac{l_{\text{elec}}\pi}{360} \quad (10)$$

where f_{Bragg} is the chosen Bragg frequency, l_{elec} is the calculated electrical length of each transmission line resonator. In order to fit n an integer for all three resonators, the appropriate f_{Bragg} needs to be chosen accordingly. In this design, the number of sections in each resonator is 11, 12, and 11, respectively. The loading capacitance C_{var} is 12 ~ 13 fF when no bias voltage is applied.

This circuit is also simulated in HP-ADS using parameter values provided above. An optimistic tuning factor of 1.5 : 1 for all MEMS capacitors is assumed. Simulated S -parameters results at 12 fF, 15 fF, and 18 fF loading MEMS capacitances are plotted in Figure 5(a) and (b). The simulated data show the center frequency shifts from 20.35 to 18.9 GHz when loading MEMS capacitances vary from 12 fF to 18 fF. Passband return loss is better than -10 dB for all tuning ranges. Though a tuning factor of 1.5 : 1 is assumed because of the tuning limitation set by MEMS capacitors, a wider tuning range can be expected if more sophisticated devices with higher tunability are incorporated in this design.

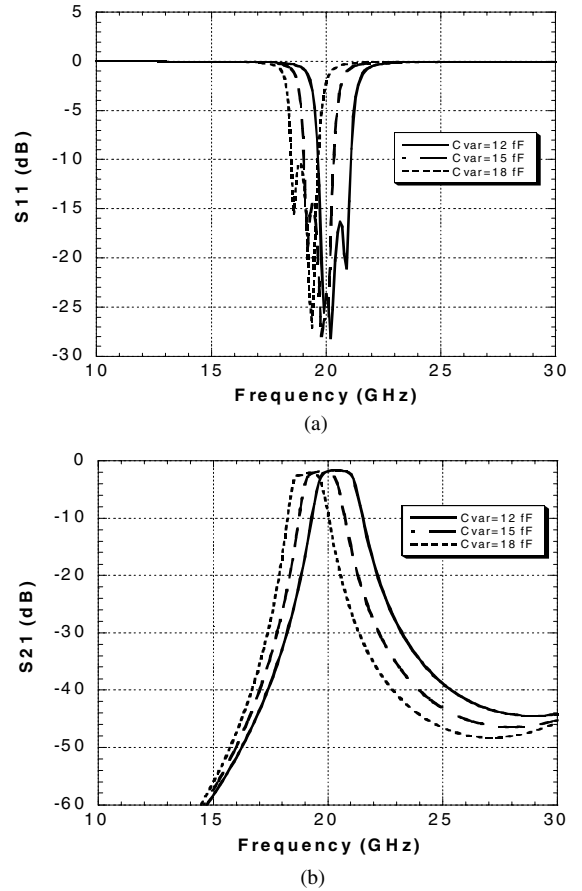


Figure 5. Simulated s -parameter of capacitively coupled MEMS tunable filter. (a) Return loss S_{11} . (b) Insertion loss S_{21} .

IV. MEASUREMENTS AND DISCUSSIONS

The three-pole capacitively coupled tunable filter was fabricated on a $700 \mu\text{m}$ thick glass substrate ($\epsilon_r = 5.7$, $\tan \delta = 0.001$) using standard IC processes. The overall filter dimension is 8.3×1.1 mm. Figure 6 is a photograph of fabricated K-band three-pole MEMS tunable bandpass filter. The coplanar waveguide is $1\text{-}\mu\text{m}$ -thick evaporated gold with central signal line width equals $150 \mu\text{m}$. Ground-to-ground spacing is $300 \mu\text{m}$. The resistive biasing network is connected to signal lines of each resonator. A bias resistor of $6 \text{K}\Omega$ is used in each bias path to isolate the DC and RF signals. A 6000\AA plasma-enhanced chemical vapor deposition (PECVD) silicon nitride layer is deposited at 290°C chamber temperature and patterned on top. Next, $1.5 \mu\text{m}$ top gold contact for MIM coupling capacitors is evaporated. In order to have 12 ~ 13 fF up state capacitance for each

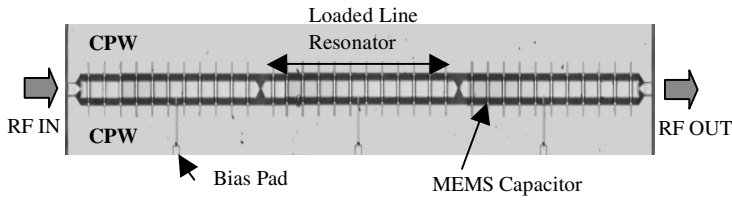


Figure 6. Photograph of fabricated three-pole MEMS tunable bandpass filter with DMTL resonators.

MEMS capacitor, a $3\text{-}\mu\text{m}$ -thick sacrificial photoresist layer, which determines the height of the MEMS airbridge, is patterned. A 20 min reflow bake on 250°C hotplate is taken to smooth the edge of patterned sacrificial photoresist. The top metal membrane is formed by evaporating a $200/30000\text{ \AA}$ Ti/Al layer on top of the sacrificial layer. The sacrificial photoresist is then removed and a critical point drying system is used to release the MEMS bridges. The width and the span of the membranes are 30 and $240\text{ }\mu\text{m}$, respectively. One important factor that needs to be addressed is the planarization of the sacrificial layer, which is critical to determine the ductile strength of MEMS airbridges. Instead of having the posts of airbridges sit on top of the ground pad, airbridges are made shorter so that the posts are moved closer to the signal line and sit on substrate between signal and ground pads. Besides, since it is risky to design a MEMS switch with a length longer than $300\text{ }\mu\text{m}$, the new structure shrinks the airbridge length to $240\text{ }\mu\text{m}$, which makes MEMS devices steadier and more reliable. Figure 7 shows the SEM microphotographs of fabricated tunable filter and well-planarized MEMS airbridge structure.

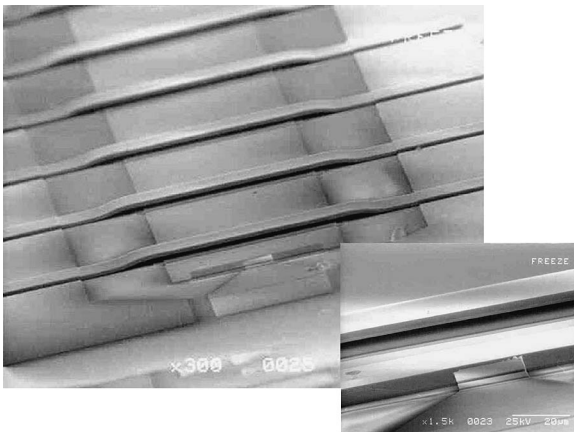
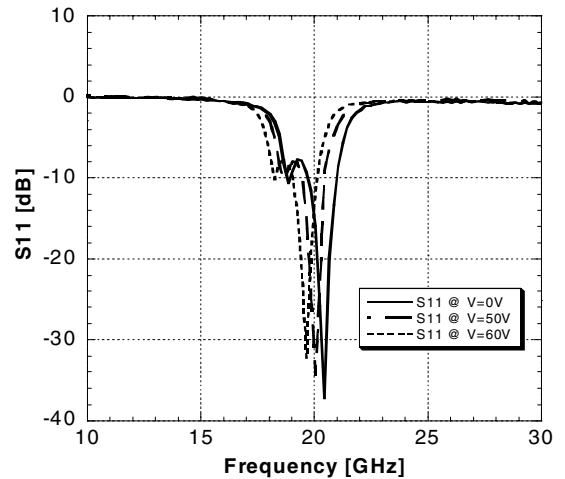
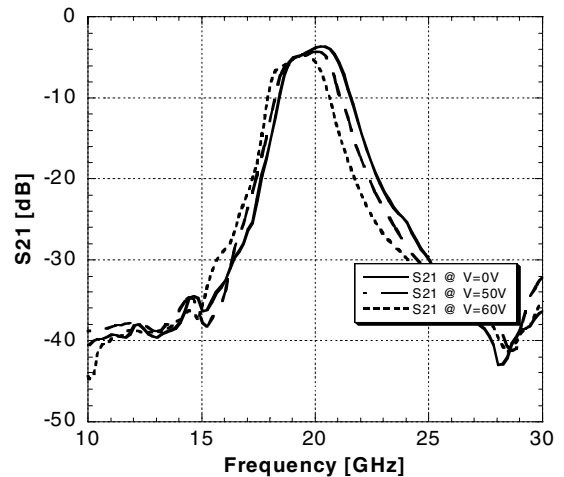


Figure 7. SEM microphotographs of fabricated tunable filter and MEMS airbridge structure.

RF measurements were made on a HP 8722D network analyzer, calibrated using on-wafer standards with $150\text{ }\mu\text{m}$ pitch coplanar Picoprobes. The two-port s -parameters of the circuit were recorded up to 30 GHz . A DC probe is connected to bias pad in order to tune each MEMS device. Figure 8 illustrates the measured S -parameters



(a)



(b)

Figure 8. Measured s -parameter of capacitively coupled MEMS tunable filter. (a) Return loss S_{11} . (b) Insertion loss S_{21} .

for MEMS variable capacitors controlled by a bias voltage of up to 60 V. The measured results demonstrate a 3.8% tuning range at 20 GHz with 3.6 dB minimum insertion losses. The relative 3 dB bandwidth increased from the designed value of 9 to 12%, which is considered to be due to process variation that makes coupling MIM capacitances larger than designed values. The out-of-band rejection at 15 and 25 GHz are -36.3 and -30.1 dB, respectively. Return loss varies from -36 to -8 dB in passband at all tuning ranges. Compared with simulated data, the difference of insertion loss in passband is about 2 dB which is considered to be unaccounted loss from substrate leakage and radiation. Using micromachined substrate and antiradiation metal cover can further reduce these losses. Since silicon nitride layer in each MEMS device is about 6000 Å thick in order to be fit into the same PECVD process as the coupling MIM capacitors, the snap-down voltage for MEMS airbridges is about 65 V, which is relatively higher than reported actuation voltage by other researchers and can be decreased by using a thinner dielectric layer.

The tuning factor of each MEMS variable capacitor is also extracted from measurements. This can be done by taking two-port S -parameter measurement of a DMTL section. Variation of MEMS capacitance will modify both magnitude and phase information of measured S -parameters, which can then be used to extract a tuning factor of each MEMS device. A detailed extraction method can be found in Ref. [8] and similar techniques have already been used to design analog and digital MEMS based phase shifters [7, 10]. With 60 V bias voltages, tuning factor of 1.27:1 is extracted from measured data, which is lower than what we expected in simulation. With further improvements in MEMS devices, it is expected to see wider tuning range of tunable filter, which can potentially be widely used in modern mm-wave radar and communication systems.

V. CONCLUSIONS

In summary, a distributed MEMS transmission line (DMTL) is investigated for mm-wave tuning circuit applications. The principle of operation of a DMTL and DMTL-based resonator is described. DMTL tunable resonators demonstrate a wide tuning range of resonant frequency with respect to the variation of loading MEMS capaci-

tance, which is desirable in mm-wave tunable filter applications. A K-band three-DMTL-resonator bandpass tunable filter is designed, fabricated, and tested on glass substrate using MEMS variable capacitors. The measured results demonstrate a 3.8% tuning range at 20 GHz with 3.6 dB minimum insertion loss. The out-of-band rejection at 15 GHz and 25 GHz are -36.3 and -30.1 dB, respectively. Return loss varies from -36 to -8 dB in passband at all tuning ranges. Additional insertion losses from measured data are attributed to unaccounted substrate leakage and radiation loss, which can be alleviated by micromachining the substrate and using antiradiation metal cover. Although currently not comparable to available commercial filters, the MEMS approach in this paper can potentially be used to implement high performance tunable filters in the future. In addition, this type of integrated tunable filter is compact, low cost and easy to process, which makes it a competitive approach in tunable filter applications.

REFERENCES

1. C. Goldsmith, T.H. Lin, B. Powers, W.R. Wu, and B. Norvell, Micromechanical membrane switches for microwave applications, 1995 IEEE MTT-S Dig, 91–94.
2. C. Goldsmith, J. Randall, S. Eshelman, T.H. Lin, D. Denniston, S. Chen, and B. Norvell, Characteristics of micromachined switches at microwave frequencies, 1996 IEEE MTT-S Dig, 1141–1144.
3. E. Brown, RF-MEMS switches for reconfigurable integrated circuits, IEEE Trans Microwave Theory Tech 46 (1998), 1868–1880.
4. E.K. Chan, E.C. Kan, R.W. Dutton, and P.M. Pinsky, Nonlinear dynamic modeling of micromachined switches, 1997 IEEE MTT-S Dig, 1511–1514.
5. J. Uher and W.J.R. Hoefer, Tunable microwave and millimeter-wave band-pass filters, IEEE Trans Microwave Theory Tech 39 (1991), 643–653.
6. H.-T. Kim, J.-H. Park, Y.-K. Kim, and Y. Kwon, Millimeter-wave micromachined tunable filters, 1999 IEEE MTT-S Dig, 1235–1238.
7. N.S. Barker and G.M. Rebeiz, Optimization of distributed MEMS phase shifters, 1999 IEEE MTT-S Dig, 299–302.
8. A.S. Nagra and R.A. York, Distributed analog phase shifters with low insertion loss, IEEE Trans Microwave Theory and Tech 47 (1999), 1705–1711.
9. G.L. Matthaei, L. Young, and E.M.T. Jones, Microwave filters, impedance matching networks and coupling structures, McGraw-Hill, New York, 1964.

10. Y. Liu, A. Borgioli, A.S. Nagra, and R.A. York, K-band three-bit low-loss distributed MEMS phase

shifter, *IEEE Microwave Guide Wave Lett* 10 (2000), 415–417.

BIOGRAPHIES



Yu Liu was born in Shenyang, China, in 1975. He received the B.S.E.E. from Tsinghua University, China, in 1998 and the M.S.E.E. degree from the University of California, Santa Barbara, in 2000. He is currently pursuing a Ph.D. in electrical and computer engineering in University of California, Santa Barbara. His present research involves applying microelectromechanical techniques and ferroelectric materials to achieve low-loss and high-performance control circuits for microwave and millimeter-wave communication systems.

Andrea Borgioli photo and biography not available.

Amit S. Nagra photo and biography not available.



Robert A. York received the B.S. degree in electrical engineering from the University of New Hampshire, Durham, in 1987 and the M.S. and Ph.D. degrees in electrical engineering from Cornell University, Ithaca, NY, in 1989 and 1991, respectively. He is currently an Associate Professor of Electrical and Computer Engineering at the University of California, Santa Barbara (UCSB). His group at UCSB is currently involved with the design and fabrication of novel microwave and millimeter-wave circuits, microwave photonics, high-power microwave and millimeter-wave modules using spatial combining and wide-bandgap semiconductor devices, and application of ferroelectric materials to microwave and millimeter-wave circuits and systems. Dr. York received the 1993 Army Research Office Young Investigator Award and the 1996 Office of Naval Research Young Investigator Award.